Int. J. Nonlinear Anal. Appl. In Press, 1–12
ISSN: 2008-6822 (electronic)
http://dx.doi.org/10.22075/ijnaa.2024.31829.4722

Global asymptotic stability of a networked fractional SIR model

Jiaming Li, Ao Huang, Yajing Li*, Hongtao Fan, Jiawei Hao, Huiyuan Wang, Jiaping Cui

College of Science, Northwest A&F University, Yangling 712100, Shaanxi, P.R. China

(Communicated by Abdolrahman Razani)

Abstract

In this paper, we consider a networked fractional SIR model. After proving the existence and uniqueness of the solution, we obtain the basic reproduction number, the disease-free equilibrium point and the endemic equilibrium point. By constructing the Lyapunov function, we show that the endemic equilibrium is globally asymptotically stable when the basic reproduction number is greater than 1, and the disease-free equilibrium is globally asymptotically stable when the basic reproduction number is less than 1. Finally, numerical simulations are carried out to verify these theoretical results. Thus, the stability theory of Laplacian diffusion is extended to the graph Laplacian model.

Keywords: Fractional SIR model, Network, Graph Laplacian operator, Global asymptotic stability, Lyapunov function
2020 MSC: 35R11, 35B40, 92D30

1 Introduction

In the past few years, many new infectious diseases have emerged worldwide, which have spread rapidly in a short period of time and caused serious impacts on human health and socio-economic development. To effectively prevent and control the spread of these diseases, establishing mathematical models has become a powerful and efficient method that can help us study the speed, impact, and dynamic change mechanisms of disease transmission. As early as the 1930s, scholars began to use mathematical models to study infectious disease dynamics. Classical models of infectious diseases were originally established in the form of ordinary differential equations. For example, the classical SIR model for endemic diseases was developed in [7]. Based on this model, a modified version of the SIR model for hepatitis B virus transmission was established in [9], as follows.

$$\begin{cases} S' = \lambda - \gamma SI - (\mu_0 + \nu)S, \\ I' = \gamma SI - (\mu_0 + \mu_1 + \beta)I, \\ R' = \beta I + \nu S - \mu_0 R, \end{cases} \tag{1.1}$$

where S, I and R represent the susceptible, infectious and recovered group, respectively. λ is the birth rate. The contact rate between susceptible population and infected population is denoted by γ. The disease induced death rate, the natural death rate and recovery rate are represented by μ_1, μ_0 and β, respectively. The vaccination rate is ν. All new births go to the susceptible class only. Recovered population has permanent immunity. Successfully vaccinated population goes to recovered population.

*Corresponding author
Email address: liyj18@nwafu.edu.com (Yajing Li)

Received: September 2023 *Accepted:* February 2024

Although (1.1) has significant limitations, its importance as the historical starting point for the development of the entire infectious disease model cannot be overstated. In order to break through the limitations imposed by integer-order derivatives, fractional derivatives were proposed [13], whose main features can be briefly summarized as follows: reflecting memory effects, capturing fractals, multi-scale properties and better data fitting. In contrast to classical models, fractional epidemic models provide powerful tools for combining memory and genetic properties of the system, such as the main features of immune responses that involve memory [15], whereas classical models ignore or make it difficult to combine such effects. The presence of memory terms in such models not only takes into account the history of the processes involved, but also has implications for the current and future development of the processes, which makes fractional models more consistent with real phenomena than integer-order classical models, since any real dynamic system depends on the history of its past states. In addition, fractional models have one more degree of freedom than classical models when fitting data. Thus, we can adapt the model to the actual data and thus better predict the evolution of the disease. In recent years, scholars have developed a variety of fractional infectious disease models based on different viral transmissions and have studied the dynamics of the models [4, 1, 2, 5, 3].

By introducing fractional order derivatives into (1.1), the authors in [6] developed a fractional order SIR model of the following form:

$$\begin{cases} {}_0^C D_t^\alpha S(t) = \lambda^\alpha - \gamma^\alpha SI - (\mu_0^\alpha + \nu^\alpha)S, \\ {}_0^C D_t^\alpha I(t) = \gamma^\alpha SI - (\mu_0^\alpha + \mu_1^\alpha + \beta^\alpha)I, \\ {}_0^C D_t^\alpha R(t) = \beta^\alpha I + \nu^\alpha S - \mu_0^\alpha R, \end{cases} \tag{1.2}$$

where the Caputo fractional derivative of order $\alpha \in (0,1)$ with the lower limit 0 for a function f is defined as

$${}_0^C D_t^\alpha f(t) = \frac{1}{\Gamma(1-\alpha)} \int_0^t (t-\tau)^{-\alpha} \frac{df}{d\tau}(\tau) \mathrm{d}\tau, \qquad t > 0,$$

and here $\Gamma(\cdot)$ denotes the Gamma function. The parameters of the model (1.2) correspond to those of model (1.1), and these modified parameters, for example λ^α, depend on the fractional order α. It is worth noting that there are several definitions of fractional derivatives, and here the Caputo fractional derivative was chosen to be used [8]. The main advantage of using the Caputo fractional derivative is that the initial conditions for fractional differential equations with Caputo derivatives are the same as those for integer order differential equations, avoiding solvability problems.

In addition, in reality, the movement of people often has an impact on the spread of disease. The movement of people within a city usually constitutes a complex network connecting cities. Epidemic spread in heterogeneous grids has been extensively studied in the last two decades [12], and these models usually do not contain weighted maps, i.e., they assume that the number of people between each city is constant, which is clearly not the case. Recently, in order to study the phenomenon of migration diffusion of populations between different cities, Tian et al. introduced weighted graphs in [17, 10, 16] and studied the propagation dynamics of networked SIR, SIRS and SEIR epidemic models. To the best of our knowledge, no one has introduced a graph Laplace operator in a fractional SIR epidemic model to study the phenomenon of population migration and diffusion between different cities. Inspired by this, we consider a networked fractional SIR model of the following form:

$$\begin{cases} {}_0^C D_t^\alpha S(t,x) - d_1^\alpha \Delta_\omega S(t,x) = \lambda^\alpha - \gamma^\alpha S(t,x)I(t,x) - (\mu_0^\alpha + \nu^\alpha)S(t,x), \quad (t,x) \in (0,+\infty) \times V, \\ {}_0^C D_t^\alpha I(t,x) - d_2^\alpha \Delta_\omega I(t,x) = \gamma^\alpha S(t,x)I(t,x) - (\mu_0^\alpha + \mu_1^\alpha + \beta^\alpha)I(t,x), \quad (t,x) \in (0,+\infty) \times V, \\ {}_0^C D_t^\alpha R(t,x) - d_3^\alpha \Delta_\omega R(t,x) = \beta^\alpha I(t,x) + \nu^\alpha S(t,x) - \mu_0^\alpha R(t,x), \quad (t,x) \in (0,+\infty) \times V, \\ S(0,x) = S_0(x) \geq (\not\equiv) 0, I(0,x) = I_0(x) \geq (\not\equiv) 0, R(0,x) = R_0(x) \geq (\not\equiv) 0, \quad x \in V, \end{cases} \tag{1.3}$$

where V is a vertices of a graph, d_i^α (i=1,2,3) is the diffusion rate of individuals among vertices dependent on the fractional order α, and Δ_ω is the graph Laplacian operator defined in (1.5).

From a mathematical point of view, a network is a graph $G = (V, E)$ consisting of vertices $V = \{1, 2, ..., n\}$ and edges set E. If vertex y is adjacent to vertex x, it is denoted as $y \sim x$. A graph is weighted if each adjacent x and y is assigned a weight ω_{xy}, where $\omega : V \times V \to [0, \infty)$ is a function satisfying that $\omega_{xy} = \omega_{yx}$ and $\omega_{xy} > 0$ if and only if $x \sim y$. Further, we define the graph differential operator D_ω as

$$D_\omega x := \sum_{y \sim x, y \in V} \omega(x, y), \tag{1.4}$$

and the graph Laplacian operator Δ_ω as

$$\Delta_\omega f(x) := \sum_{y \sim x, y \in V} (f(y) - f(x))\omega(x, y), \tag{1.5}$$

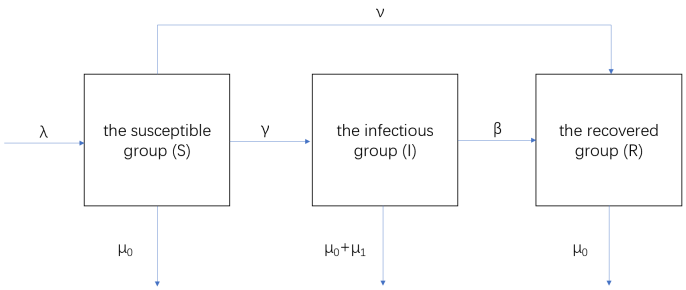

Figure 1: Model flow chart

where $f : V \to \mathbb{R}$.

In particular, when the order of the fractional derivative $\alpha = 1$, the model degenerates to the classical model, and the global asymptotic stability of the disease-free and endemic equilibrium points is also studied in [17, 10]. Therefore, our goal is to generalize the stability theory of the classical integer-order networked SIR model to the corresponding fractional-order model.

2 Existence and uniqueness

This is obvious because the number of susceptible people is non-negative when an epidemic occurs, and the number of infected people is non-negative if, and only if, the number of susceptible people is zero, or the number of infected people is zero.

By applying Theorem 3.1 and Remark 3.2 in [11], we can obtain the existence and uniqueness of the solution.

Theorem 2.1. The system (1.3) has a unique solution.

3 The equilibrium point and basic reproduction number

The basic reproduction number is the number of new infections (the number of second generation cases that can be infected) that can be produced by a case entering a susceptible population under ideal conditions. We'll call it $\mathcal{R}_0$ here. When $\mathcal{R}_0$ is greater than 1, then the infection can spread through the whole crowd, become a pandemic, but less vulnerable groups, part of the infected people died of the infection. The possibility that parts of the population may develop immunity after recovering from the disease and vaccination against the infection mean that infections do not generally last forever when the $\mathcal{R}_0$ is less than 1, infectious diseases will gradually disappear. The system for determining the equilibrium is as follows:

$$\begin{cases} d_1^\alpha \Delta_\omega S + \lambda^\alpha - \gamma^\alpha SI - (\mu_0^\alpha + \nu^\alpha)S = 0, \\ d_2^\alpha \Delta_\omega I + \gamma^\alpha SI - (\mu_0^\alpha + \mu_1^\alpha + \beta^\alpha)I = 0, \\ d_3^\alpha \Delta_\omega R + \beta^\alpha I + \nu^\alpha S - \mu_0^\alpha R = 0. \end{cases} \tag{3.1}$$

According to literature [17], this system is equivalent to the following system:

$$\begin{cases} \lambda^\alpha - \gamma^\alpha SI - (\mu_0^\alpha + \nu^\alpha)S = 0, \\ \gamma^\alpha SI - (\mu_0^\alpha + \mu_1^\alpha + \beta^\alpha)I = 0, \\ \beta^\alpha I + \nu^\alpha S - \mu_0^\alpha R = 0. \end{cases} \tag{3.2}$$

Thus by solving the system (3.2) and according to the basic reproduction number theorem, we obtain the following theorems.

Theorem 3.1. When $\mathcal{R}_0 < 1$, the system(1.3) has a unique disease-free equilibrium point $E_0 = \left(\frac{\lambda^\alpha}{\mu_0^\alpha + \nu^\alpha}, 0, \frac{\nu^\alpha \lambda^\alpha}{\mu_0^\alpha(\mu_0^\alpha + \nu^\alpha)}\right)$.

Theorem 3.2. When $\mathcal{R}_0 > 1$, the system(1.3) has a unique endemic equilibrium point $E_1 = (S^*, I^*, R^*)$, where $S^* = \frac{\mu_0^\alpha + \mu_1^\alpha + \beta^\alpha}{\gamma^\alpha}, I^* = \frac{\lambda^\alpha \nu^\alpha - (\mu_0^\alpha + \mu_1^\alpha + \beta^\alpha)(\mu_0^\alpha + \nu^\alpha)}{(\mu_0^\alpha + \mu_1^\alpha + \beta^\alpha)\gamma^\alpha}, R^* = \frac{\beta^\alpha I^* + \nu^\alpha S^*}{\mu_0^\alpha}$.

Next, we calculate the basic reproduction number $\mathcal{R}_0$ according to [18]. Let

$$\mathscr{F} = \begin{bmatrix} \gamma^\alpha SI \\ 0 \\ 0 \end{bmatrix} = \begin{bmatrix} \mathscr{F}_1 \\ 0 \\ 0 \end{bmatrix}$$

be the rate of appearance of new infections in compartment I, S, R, and

$$\mathscr{V} = \begin{bmatrix} (\mu_0^\alpha + \mu_1^\alpha + \beta^\alpha)I \\ -\lambda^\alpha + \gamma^\alpha SI + (\mu_0^\alpha + \nu^\alpha)I \\ \mu_0^\alpha R - \beta^\alpha I - \upsilon^\alpha S \end{bmatrix} = \begin{bmatrix} \mathscr{V}_1 \\ \mathscr{V}_2 \\ \mathscr{V}_3 \end{bmatrix}$$

be the rate of change of the individual in compartment I, S, R by all other means. Then we have $F = \left[\frac{\partial \mathscr{F}_1}{\partial I} \mid_{E_0}\right] = \left[\gamma^\alpha S \mid_{E_0}\right] = \left[\frac{\gamma^\alpha \lambda^\alpha}{\mu_0^\alpha + \nu^\alpha}\right]$, and $V = \left[\frac{\partial \mathscr{V}_1}{\partial I} \mid_{E_0}\right] = \left[\mu_0^\alpha + \mu_1^\alpha + \beta^\alpha\right]$. Then we obtain the basic reproduction number

$$\mathcal{R}_0 = FV^{-1} = \frac{\gamma^\alpha \lambda^\alpha}{(\mu_0^\alpha + \mu_1^\alpha + \beta^\alpha)(\mu_0^\alpha + \upsilon^\alpha)}. \tag{3.3}$$

It should be noted that when the order of the fractional derivative $\alpha \to 1$ in (1.3), the expression for the basic reproduction number in (3.3) degenerates to the result in [17].

4 Local stability of the equilibria

Theorem 4.1. If $\mathcal{R}_0 < 1$, the disease-free equilibrium E_0 of (1.3) is locally asymptotically stable, while if $\mathcal{R}_0 > 1$, then E_0 is unstable.

Proof . The Jacobian matrix of the system (1.3) at E_0 is

$$J|_{E_0} = \begin{bmatrix} -(\mu_0^\alpha + \nu^\alpha) & -\frac{\gamma^\alpha \lambda^\alpha}{\mu_0^\alpha + \nu^\alpha} & 0 \\ 0 & \frac{\gamma^\alpha \lambda^\alpha}{\mu_0^\alpha + \nu^\alpha} - (\mu_0^\alpha + \mu_1^\alpha + \beta^\alpha) & 0 \\ \nu^\alpha & \beta^\alpha & -\mu_0^\alpha \end{bmatrix}.$$

Based on $\|\lambda I - J|_{E_0}\| = 0$, we can find that the eigenvalues of the matrix are $\lambda_1 = -\mu_0^\alpha$, $\lambda_2 = -(\mu_0^\alpha + \nu^\alpha)$, and $\lambda_3 = \frac{\gamma^\alpha \lambda^\alpha}{\mu_0^\alpha + \nu^\alpha} - (\mu_0^\alpha + \mu_1^\alpha + \beta^\alpha) = (\mu_0^\alpha + \mu_1^\alpha + \beta^\alpha)[\mathcal{R}_0 - 1]$. So, λ_1, λ_2 both are negative, and the third eigenvalue λ_3 depends on the $\mathcal{R}_0$. It can be concluded that all three eigenvalues of $J|_{E_0}$ are negative if and only if $\mathcal{R}_0 < 1$. Thus system (1.3) is locally asymptotically stable around E_0. If $\mathcal{R}_0 > 1$, then λ_3 is positive and two other eigenvalues are negative, so we conclude that E_0 is unstable. □

Theorem 4.2. The endemic equilibrium point E_1 of the system (1.3) is locally asymptotically stable if $\mathcal{R}_0 > 1$.

Proof . The Jacobian matrix of the system (1.3) at E_1 is

$$J|_{E_1} = \begin{bmatrix} -\frac{\gamma^\alpha \lambda^\alpha}{\mu_0^\alpha + \mu_1^\alpha + \nu^\alpha} & -(\mu_0^\alpha + \mu_1^\alpha + \beta^\alpha) & 0 \\ \frac{\gamma^\alpha \lambda^\alpha - (\mu_0^\alpha + \mu_1^\alpha + \beta^\alpha)(\mu_0^\alpha + \nu^\alpha)}{\mu_0^\alpha + \mu_1^\alpha + \beta^\alpha} & 0 & 0 \\ \nu^\alpha & \beta^\alpha & -\mu_0^\alpha \end{bmatrix}.$$

One of the eigenvalues of $J|_{E_1}$ is $\lambda_1 = -\mu_0^\alpha$. To calculate other eigenvalues, we consider the following matrix:

$$P_0 = \begin{bmatrix} -\dfrac{\gamma^\alpha \lambda^\alpha}{\mu_0^\alpha + \mu_1^\alpha + \nu^\alpha} & -(\mu_0^\alpha + \mu_1^\alpha + \beta^\alpha) \\ \dfrac{\gamma^\alpha \lambda^\alpha - (\mu_0^\alpha + \mu_1^\alpha + \beta^\alpha)(\mu_0^\alpha + \nu^\alpha)}{\mu_0^\alpha + \mu_1^\alpha + \beta^\alpha} & 0 \end{bmatrix}.$$

Then we can obtain that

$$trace(P_0) = -\frac{\gamma^\alpha \lambda^\alpha}{\mu_0^\alpha + \mu_1^\alpha + \nu^\alpha} < 0,$$

and

$$det(P_0) = [\gamma^\alpha \lambda^\alpha - (\mu_0^\alpha + \mu_1^\alpha + \beta^\alpha)(\mu_0^\alpha + \nu^\alpha)] = [(\mu_0^\alpha + \mu_1^\alpha + \beta^\alpha)(\mu_0^\alpha + \nu^\alpha)][\mathcal{R}_0 - 1].$$

When $\mathcal{R}_0 > 1$, we have $det(P_0) > 0$. So E_1 is locally asymptotically stable if $\mathcal{R}_0 > 1$. □

5 Global stability of the equilibria

Theorem 5.1. If $\mathcal{R}_0 < 1$ and $S + I + R \leq \frac{\lambda^\alpha}{\mu_0^\alpha + \nu^\alpha}$, then the disease-free equilibrium E_0 of the system (1.3) is globally asymptotically stable.

Proof . The Lyapunov function $L(t)$ is defined by $L(t) = \frac{1}{2}\sum_{x\in\mathbb{V}} I^2 + \frac{1}{2}\sum_{x\in\mathbb{V}} \left(S + I + R - \frac{\lambda^\alpha}{\mu^\alpha}\right)^2$. From Lemma 2.4(a) in [5] and (1.3) , it follows that

$$\begin{aligned} {}_0^C D_t^\alpha L(t) &\leq \sum_{x\in\mathbb{V}} I \left({}_0^C D_t^\alpha I\right) + \sum_{x\in\mathbb{V}} \left(S + I + R - \frac{\lambda^\alpha}{\mu^\alpha}\right) {}_0^C D_t^\alpha \left(S + I + R - \frac{\lambda^\alpha}{\mu^\alpha}\right) \\ &\leq \sum_{x\in\mathbb{V}} I[d_2^\alpha \Delta_\omega I + \gamma^\alpha SI - (\mu_0^\alpha + \mu_1^\alpha + \beta^\alpha)I] + \sum_{x\in\mathbb{V}} \left(S + I + R - \frac{\lambda^\alpha}{\mu^\alpha}\right) \\ &\qquad \times [d_1^\alpha \Delta_\omega S + d_2^\alpha \Delta_\omega I + d_3^\alpha \Delta_\omega R + \lambda^\alpha - \mu_0^\alpha (S + I + R) - \mu_1^\alpha I]. \end{aligned} \tag{5.1}$$

By Lemma 2.1 in [17], we can remove the terms with Laplacian in (5.1). Then, we have

$${}_0^C D_t^\alpha L(t) \leq \sum_{x\in\mathbb{V}} I[\gamma^\alpha SI - (\mu_0^\alpha + \mu_1^\alpha + \beta^\alpha)I] + \sum_{x\in\mathbb{V}} \left(S + I + R - \frac{\lambda^\alpha}{\mu^\alpha}\right)[\lambda^\alpha - \mu_0^\alpha (S + I + R) - \mu_1^\alpha I]. \tag{5.2}$$

From the condition $S + I + R \leq \dfrac{\lambda^\alpha}{\mu_0^\alpha + \nu^\alpha}$, it can be deduced that $S \leq \dfrac{\lambda^\alpha}{\mu_0^\alpha + \nu^\alpha}$ and $S + I + R \leq \dfrac{\lambda^\alpha}{\mu_0^\alpha}$. Using $\mathcal{R}_0 < 1$, we can get that

$$\begin{aligned} {}_0^C D_t^\alpha L(t) &\leq \sum_{x\in\mathbb{V}} I^2 \left[\frac{\gamma^\alpha \lambda^\alpha}{\mu_0^\alpha + \nu^\alpha} - (\mu_0^\alpha + \mu_1^\alpha + \beta^\alpha)\right] + \sum_{x\in\mathbb{V}} \left(S + I + R - \frac{\lambda^\alpha}{\mu^\alpha}\right)[\lambda^\alpha - \mu_0^\alpha (S + I + R) - \mu_1^\alpha I] \\ &\leq \sum_{x\in\mathbb{V}} I^2 (\mu_0^\alpha + \mu_1^\alpha + \beta^\alpha) \left[\frac{\gamma^\alpha \lambda^\alpha}{(\mu_0^\alpha + \mu_1^\alpha + \beta^\alpha)(\mu_0^\alpha + v^\alpha)} - 1\right] \\ &\quad + \sum_{x\in\mathbb{V}} \frac{\mu_1^\alpha}{\mu_0^\alpha} I \left(S + I + R - \frac{\lambda^\alpha}{\mu^\alpha}\right) - \mu_0^\alpha \left(S + I + R - \frac{\lambda^\alpha}{\mu^\alpha}\right)^2 \\ &\leq 0, \end{aligned} \tag{5.3}$$

and ${}_0^C D_t^\alpha L(t) = 0$ if and only if $I = 0$ and $S + R = \dfrac{\lambda^\alpha}{\mu_0^\alpha}$. Moreover, we have $\lim\limits_{t\to\infty} S(t) = \dfrac{\lambda^\alpha}{\mu_0^\alpha + \nu^\alpha}$ and $\lim\limits_{t\to\infty} R(t) = \dfrac{\nu^\alpha \lambda^\alpha}{\mu_0^\alpha (\mu_0^\alpha + \nu^\alpha)}$. Thus, $\lim\limits_{t\to\infty} (S, I, R) = E_0$. This completes the proof. □

Theorem 5.2. If $\mathcal{R}_0 > 1$, then the endemic equilibrium E_1 of the system (1.3) is globally asymptotically stable.

Proof . Let $\phi(x) = x - 1 - \ln x$, $x > 0$. Define the Lyapunov function $L_1(t)$ by $L_1(t) = F_1(t) + F_2(t)$, where

$$F_1(t) = \sum_{x\in\mathbb{V}} S^*\phi\left(\frac{S}{S^*}\right), \quad F_2(t) = \sum_{x\in\mathbb{V}} I^*\phi\left(\frac{I}{I^*}\right).$$

Then $L_1(t) \geq 0$, for all $t \geq 0$. We assume $d_i > 0, i = 1, 2, 3$. Substituting the endemic equilibrium into (1.3), we obtain

$$\begin{cases} \lambda^\alpha = r^\alpha S^* I^* + (\mu^\alpha + \nu^\alpha)S^*, \\ \mu_0^\alpha + \mu_1^\alpha + \beta^\alpha = \gamma^\alpha S^*. \end{cases} \tag{5.4}$$

Below, we evaluate the α-th order Caputo derivatives of F_i, $i = 1, 2$. By Lemma 2.4(b) in [5], Lemma 2.1 in [17] and $\lambda^\alpha = \gamma^\alpha S^* I^* + (\mu_0^\alpha + \nu^\alpha)S^*$, we have that

$$\begin{aligned} {}_0^C D_t^\alpha F_1(t) &= {}_0^C D_t^\alpha \left(\sum_{x\in\mathbb{V}} S^*\phi\left(\frac{S}{S^*}\right)\right) \leq \sum_{x\in\mathbb{V}} \frac{S - S^*}{S} {}_0^C D_t^\alpha S \\ &= \sum_{x\in\mathbb{V}} (\lambda^\alpha - \gamma^\alpha SI - (\mu_0^\alpha + \nu^\alpha)S)\frac{S - S^*}{S} \\ &= \sum_{x\in\mathbb{V}} (\gamma^\alpha S^* I^* + (\mu_0^\alpha + \nu^\alpha)S^* - \gamma^\alpha SI - (\mu_0^\alpha + \nu^\alpha)S)\frac{S - S^*}{S} \\ &= \sum_{x\in\mathbb{V}} [(\mu_0^\alpha + \nu^\alpha + \gamma^\alpha I^*)(S^* - S) + \gamma^\alpha S(I^* - I)]\frac{S - S^*}{S} \\ &= -\sum_{x\in\mathbb{V}} \frac{(S - S^*)^2(\mu_0^\alpha + \nu^\alpha + \gamma^\alpha I^*)}{S} - \sum_{x\in\mathbb{V}} \gamma^\alpha (S - S^*)(I - I^*), \end{aligned} \tag{5.5}$$

and

$$\begin{aligned} {}_0^C D_t^\alpha F_2(t) &\leq \sum_{x\in\mathbb{V}} \frac{I - I^*}{I} {}_0^C D_t^\alpha I \leq \sum_{x\in\mathbb{V}} \frac{I - I^*}{I} [\gamma^\alpha SI - (\mu_0^\alpha + \mu_1^\alpha + \beta^\alpha)I] \\ &= \sum_{x\in\mathbb{V}} (I - I^*)(\gamma^\alpha S - \gamma^\alpha S^*) = \sum_{x\in\mathbb{V}} \gamma^\alpha (S - S^*)(I - I^*). \end{aligned} \tag{5.6}$$

Therefore,

$${}_0^C D_t^\alpha L_1(t) \leq -\sum_{x\in\mathbb{V}} \frac{((S - S^*)^2(\mu_0^\alpha + \nu^\alpha + \gamma^\alpha I^*)}{S} \leq 0. \tag{5.7}$$

Thus, ${}_0^C D_t^\alpha L_1(t) \leq 0$ and ${}_0^C D_t^\alpha L_1(t) = 0$ if and only if $S = S^*$, $I = I^*$, and $R = R^*$. This completes the proof. □

6 Numerical simulations

In order to deal with the numerical solutions of system (1.3), we denote the adjacent matrix of the graph G by $\mathcal{G}$, and take the mean number of passengers per unit time moving from x_i to x_j as the weighted matrix $(\omega_{ij})_{n\times n}$. Here we assume that $(\omega_{ij})_{n\times n}$is a symmetric matrix. Set $S(t, x) = U_1(t, i)$, $I(t, x) = U_2(t, i)$, and $R(t, x) = U_3(t, i)$, we then rewrite system(1.3) as the following ordinary differential equations:

$${}_0^C D_t^\alpha U_k(t, i) = f_k(U_1, U_2, U_3)(t, i) + d_k \sum_{j=1}^{n} L_{ij} U_k(j, t), \quad i = 1, 2, \ldots, n, \tag{6.1}$$

where $k = 1, 2, 3$. L is called the Laplacian matrix, which is defined by

$$L_{ij} = \begin{cases} \mathcal{G}_{ij}\omega_{ij}, & j \neq i, \\ -\sum\limits_{j=1}^{n} \mathcal{G}_{ij}\omega_{ij}, & j = i. \end{cases}$$

6.1 The case of $\mathcal{R}_0 < 1$

In this case, we assume an initial population of 500,000, distribute it equally over 100 nodes, i.e. an initial susceptible population of 5,000 per node, and set the initial number of infections to exist only at the first node and to be 12. Theorem 3.1 shows that the system will converge to the disease-free equilibrium point E_0 at $\mathcal{R}_0 < 1$, so we take the following parameter values (Time= $[t]$ = one day):

$$\lambda = 5, \gamma = 0.003, \beta = 0.3, \mu_0 = 0.001, \mu_1 = 0.01, \nu = 0.25$$

and the order of the fractional derivative $\alpha = 0.99$, and we assume that the graph G is a Watts-Strogatz network with 100 nodes, an average node degree of 6, and a reconnection probability of 0.25. An average degree of 6 means that each node has 3 other nodes connected to its left and right. The 0.25 probability of reconnecting a link indicates that each node has a probability of 0.25 of connecting to any other node in the figure.

In the first panel of Figure 2, we depict the initial infected population in the network, taking 12 at the first node and 0 at all other nodes. Using a fractional Euler format to integrate over time, in the other four panels of Figure 2, we plot the spatial density of the infected populations on the network at $t = 200, 400, 600, 1000$. The results show that for different nodes, the network exhibits spatially inhomogeneous behavior.

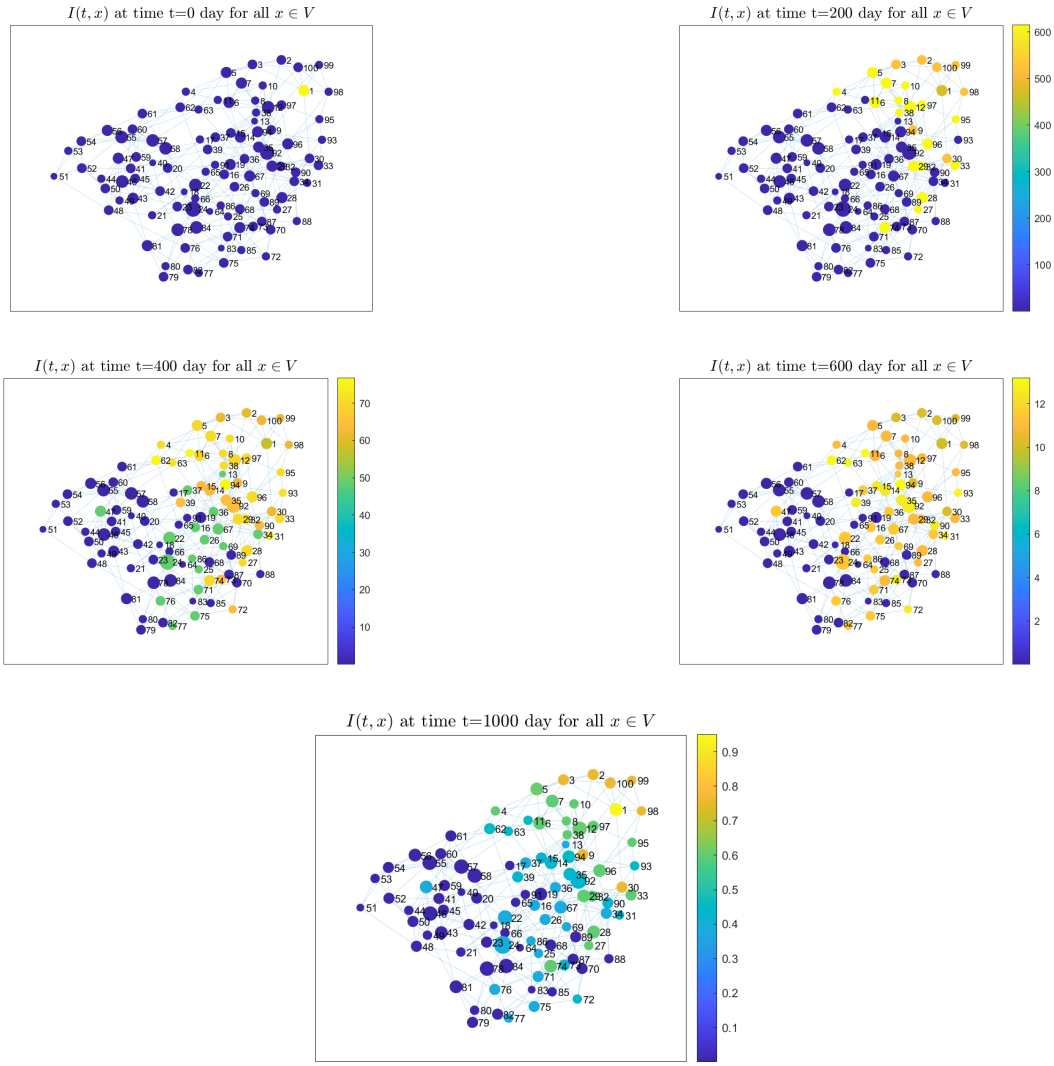

Figure 2: Solutions of I in Watts-Strogatz networks at moments $t = 0, 200, 400, 600$ and 1000. The node size corresponds to the node degree and the node colour bar corresponds to the overall.

In Figure 3, the nodes are arranged in a column without regard to their spatial location, and the trend of all nodes over time is studied. The results show that when $\mathcal{R}_0 < 1$, the number of infections basically shows a trend of rising to a peak and then continuously decreasing to 0.

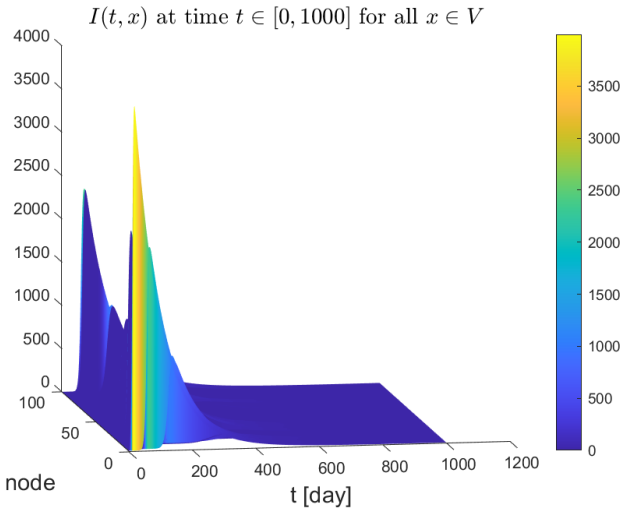

Figure 3: For $\mathcal{R}_0 < 1$, dynamical behavior of the networked fractional SIR model with $\alpha = 0.99$.

In Figure 4, we consider the dynamical behavior of the system without Laplacian diffusion, using the first node as an example to study the trend in the number of individual populations over time. The left panel shows the trend over the entire time period [0, 1000], the right panel shows the details over the time period [0, 200]. The disease-free equilibrium point of the system (1.3) is given by Theorem 3.1, i.e. $E_0 = (19.9, 0, 4980.1)$. The disease-free equilibrium point obtained by iteration at fractional order $\alpha = 0.99$ is (25.18, 0.94, 4847.9), which is basically close to the theoretical result E_0. For the corresponding integer-order model, i.e. with derivative order 1, the equilibrium value obtained by iteration is (19.79, 0.0795, 4853.5), which is closer to the theoretical result E_0 than the fractional order $\alpha = 0.99$.

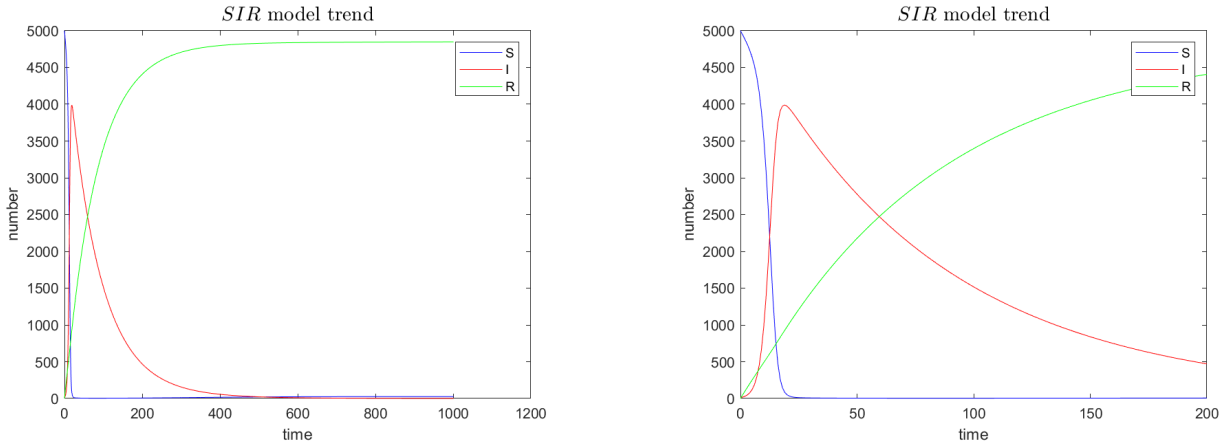

(a) $t \in [0, 1000]$ (b) $t \in [0, 200]$

Figure 4: For $\mathcal{R}_0 < 1$, dynamical behavior of the fractional order model without Laplacian diffusion at $\alpha = 0.99$.

6.2 The case of $\mathcal{R}_0 > 1$

For the model with $\mathcal{R}_0 > 1$, the initial value of the susceptible population is taken to be 200 people per node, giving a total of 20,000 people. The number of infected people at the first node is 12, and we take the parameter values (Time= $[t]$ = one day):

$$\lambda = 10, \gamma = 0.012, \beta = 0.002, \mu_0 = 0.0342, \mu_1 = 0.0136, \nu = 0.07.$$

In Figure 5, we make a portrait of the spatial densities of infected population on the network for time $t = 0, 200, 400, 600, 1000$, showing that, for different nodes, the network exhibits a spatially inhomogeneous behavior.

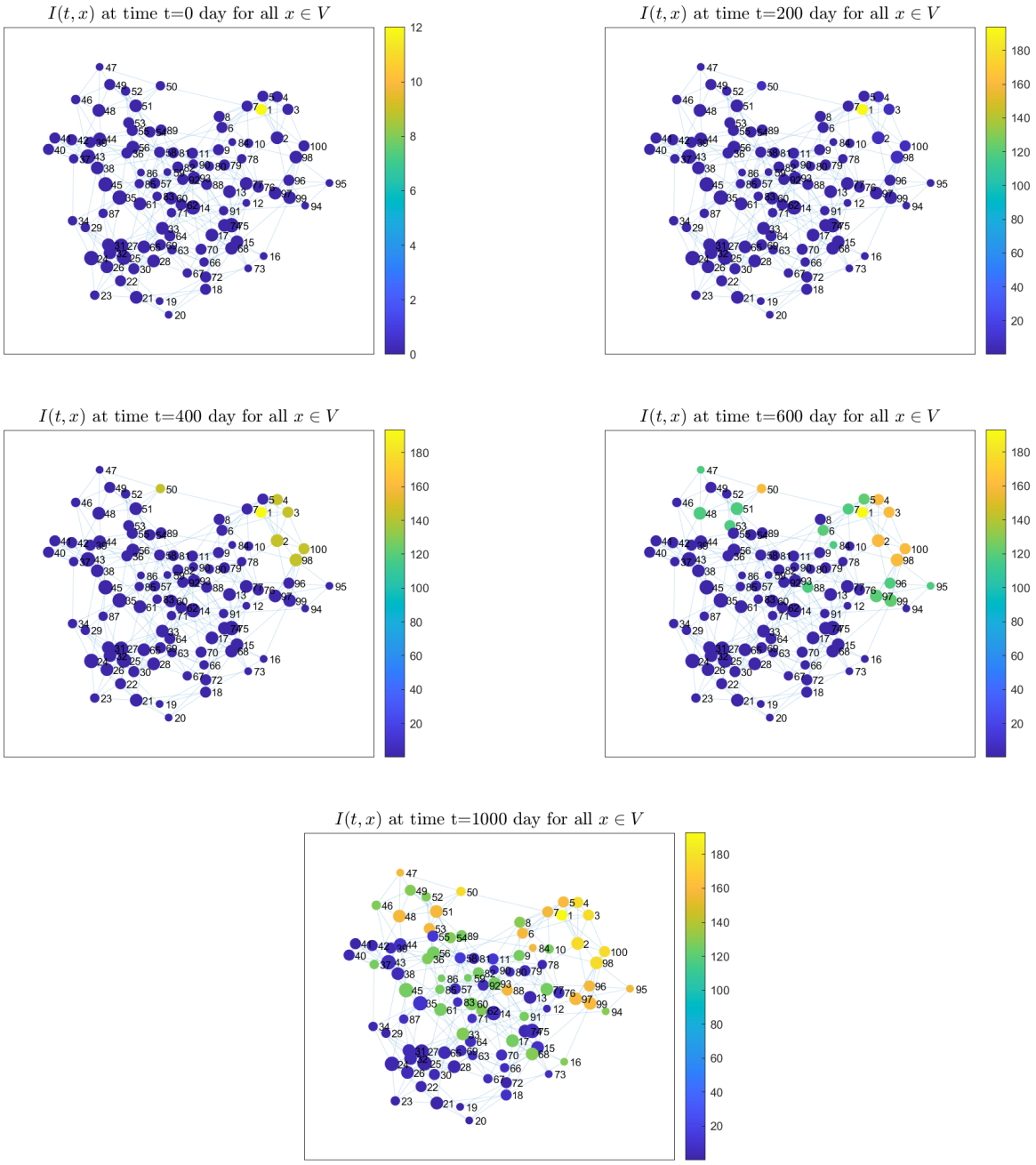

Figure 5: Solutions of I in the Watts-Strogatz network at moments $t = 0, 200, 400, 600$ and 1000 for $\mathcal{R}_0 > 1$. The node size corresponds to the node degree and the node colour bar corresponds to the overall.

Figure 6 shows the number of infections over time for all nodes with $\mathcal{R}_0 > 1$. It can be seen that the number of infections increases over time until it peaks and then reaches equilibrium at the peak. Figure 7 depicts the dynamical behavior of the system without Laplacian diffusion. The right panel shows the trend over the entire time period [0, 1000], and the left panel shows the details over the time period [0, 200]. Taking the first node as an example, we consider the trend in the number of various populations over time. The endemic equilibrium point of the system (1.3) is known from Theorem 3.2 to be $E_1 = (4.15, 192.12, 19.72)$, and the result obtained by iteration at fractional order $\alpha = 0.99$ corresponds to an equilibrium value of (4.16, 192.55, 18.74), almost identical to the theoretical result E_1.

For the corresponding integer-order model, i.e. with derivative order 1, the equilibrium value obtained by iteration is (4.14, 192.43, 18.98), which is almost identical to that obtained for the fractional-order model at $\alpha = 0.99$. This indicates that the experimental results are in agreement with the theoretical analysis.

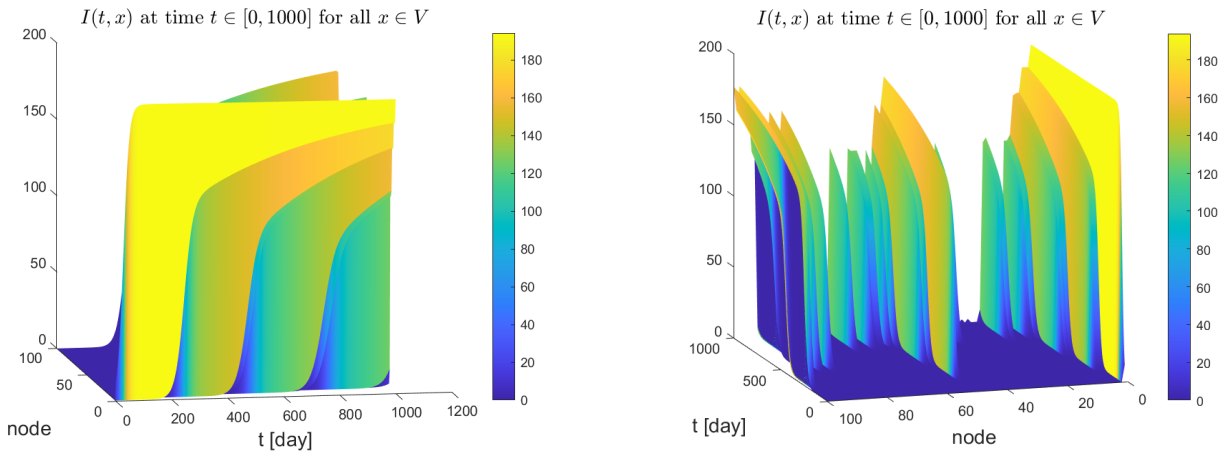

Figure 6: For $\mathcal{R}_0 > 1$, dynamical behavior of the networked fractional SIR model with $\alpha = 0.99$. The left panel is the same as the right panel, and the right panel is the other direction of the left panel.

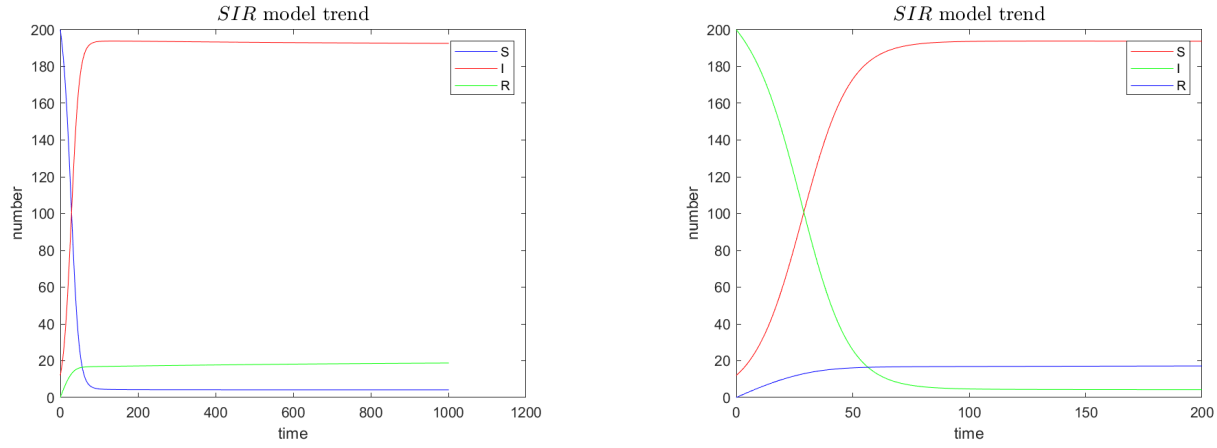

Figure 7: For $\mathcal{R}_0 > 1$, dynamical behavior of the fractional order model without Laplacian diffusion at $\alpha = 0.99$.

6.3 Effect of different fractional orders on the system

From the results obtained in Sections 6.1 and 6.2, it can be seen that the equilibrium point of the system with fractional order $\alpha = 0.99$ is similar to that of the integer order 1, and the difference between them corresponding to the overall trend graph is not obvious. Therefore, we take the number of infections at the first node as an example to study the trend of the number of infections under different fractional orders, i.e. we only consider the effect of different fractional orders on the number of infections.

As can be seen in Figure 8, when $\mathcal{R}_0 < 1$, for different fractional orders, the number of infected people reaches the peak at different moments, and as the fractional order decreases, the time to reach the peak is shortening, the peak is decreasing, and the rate of decline from the peak to 0 is increasing. As can be seen in Figure 9, when $\mathcal{R}_0 > 1$, the rate of increase in the number of infections varies as the fractional order changes. As time increases, the number of infections eventually reaches equilibrium, and the equilibrium point has different values. The above results show that the model (1.3) exhibits different dynamical behavior as the fractional order changes, and therefore the fractional order derivative models have more advantages over the traditional integer order derivative models in modelling.

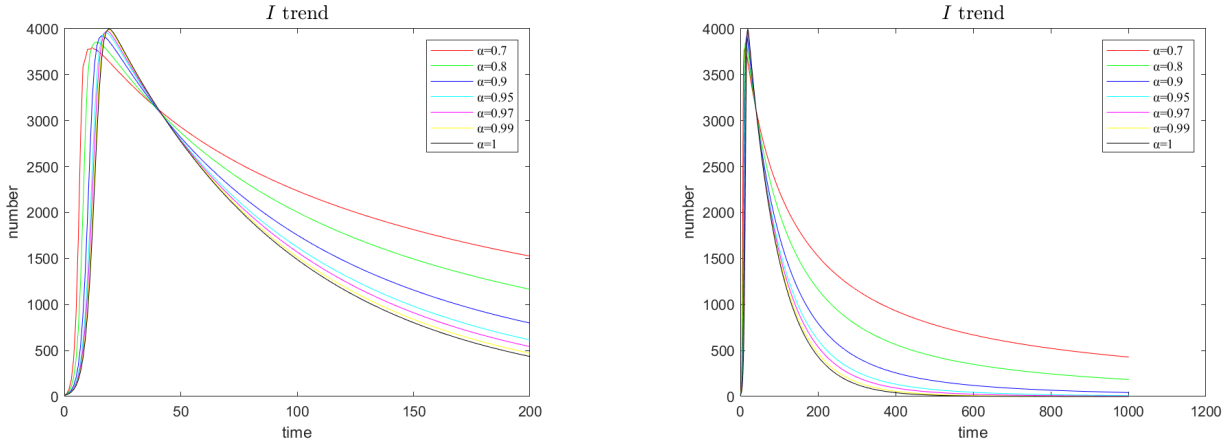

Figure 8: Trends in the number of infections at different fractional order steps for $\mathcal{R}_0 < 1$, the right panel shows the trend over the entire time period [0, 1000], the left panel shows the details over the time period [0, 200].

7 Conclusions

In this article, we first introduce a graph Laplace operator to a fractional SIR epidemic model, and prove the existence of uniqueness of the solution of this model. Then, we complete the calculation of the equilibrium point and the basic reproduction number. Next, we discuss the stability of the system, and prove the local stability and global asymptotic stability of the disease-free equilibrium point and the endemic equilibrium point using the matrix form and the method of constructing Lyapunov functions, respectively. Finally, the correctness of the theoretical analysis is verified by numerical experiments.

Declaration of Interest Statement

The authors declare that they have no known competing financial interests or personal relationships that could have appeared to influence the work reported in this paper.

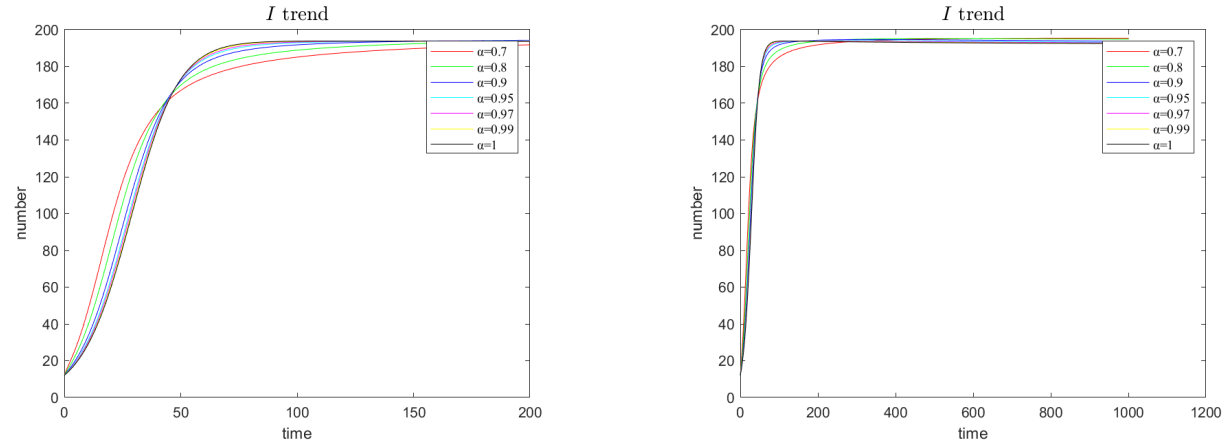

Figure 9: Trends in the number of infections at different fractional order steps for $\mathcal{R}_0 > 1$, the right panel shows the trend over the entire time period [0, 1000], the left panel shows the details over the time period [0, 200].

Acknowledgments

This work is supported by the National Natural Science Foundation of China (Nos. 11801452, 11701456), Shaanxi Fundamental Science Research Project for Mathematics and Physics (Grant No. 22JSQ020), Fundamental Research

Project of Natural Science in Shaanxi Province General Project (Youth) (Nos. 2019JQ-415, 2019JQ-196), Chinese Universities Scientific Funds (Nos. 2452022104, 2452022105, 2452022372), and Innovation and Entrepreneurship Training Program for College Students of Northwest A&F University (Nos. 202110712186, 202210712048).

References

[1] R. Almeida, *Analysis of a fractional SEIR model with treatment*, Appl. Math. Lett. **84** (2018), 56–62.

[2] R. Almeida, A.M.C. Brito da Cruz, N. Martins, M. Teresa, and T. Monteiro, *An epidemiological MSEIR model described by the Caputo fractional derivative*, Int. J. Dyn. Control **7** (2019), 776–784.

[3] Y.L. Chen, F.W. Liu, Q. Yu, and T.Z. Li, *Review of fractional epidemic models*, Appl. Math. Model. **97** (2021), 281–307.

[4] K. Diethelm, *A fractional calculus based model for the simulation of an outbreak of dengue fever*, Nonlinear Dyn. **71** (2013) 613–619.

[5] J.R. Graef, L.G. Kong, A. Ledoan, and M. Wang, *Stability analysis of a fractional online social network model*, Math. Comput. Simul. **178** (2020), 625–645.

[6] P.T. Karaji and N. Nyamoradi, *Analysis of a fractional SIR model with general incidence function*, Appl. Math. Lett. **108** (2020), 106499.

[7] W.O. Kermack and A.G. McKendrick, *A contribution to mathematical theory of epidemics*, Proc. Royal Soc. A **115** (1927), 700–721.

[8] A.A. Kilbas, H.M. Srivastava, and J.J. Trujillo, *Theory and Applications of Fractional Differential Equations*, Boston, Elsevier, 2006.

[9] T. Khan, Z. Ullah, N. Ali, and G. Zaman, *Modeling and control of the hepatitis B virus spreading using an epidemic model*, Chaos Solitons Fractals **124** (2019), 1–9.

[10] Z.H. Liu and C.R. Tian, *A weighted networked SIRS epidemic model*, J. Differ. Equ. **269** (2020), 10995–11019.

[11] W. Lin, *Global existence theory and chaos control of fractional differential equations*, J. Math. Anal. Appl. **332** (2007), 709–726.

[12] R. Pastor-Satorras, C. Castellano, P. Van Mieghem, and A. Vespignani, *Epidemic processes in complex networks*, Rev. Modern Phys. **87** (2015), 925–986.

[13] S.G. Samko, A.A. Kilbas, and O.I. Marichev, *Fractional Integrals and Derivatives*, Translated from the 1987 Russian original, Gordon and Breach, Yverdon, 1993.

[14] A. Slavik, *Lotka-Volterra competition model on graphs*, SIAM J. Appl. Dyn. Syst. **192** (2020), 725–762.

[15] A.A. Stanislavsky, *Memory effects and macroscopic manifestation of randomness*, Phys. Rev. E **61** (2008), no. 5, 4752–4759.

[16] C.R. Tian, Z.H. Liu, and S.G. Ruan, *Asymptotic and transient dynamics of SEIR epidemic models on weighted networks*, Eur. J. Appl. Math. **34** (2023), 238–261.

[17] C.R. Tian, Q.Y. Zhang, and L. Zhang, *Global stability in a networked SIR epidemic model*, Appl. Math. Lett. **107** (2020), 106444.

[18] P. Van den Driessche and J. Watmough, *Reproduction numbers and sub-threshold endmic equlibria for compartmental models of diesease transmission*, Math. Biosci. **180** (2002), 29–48.